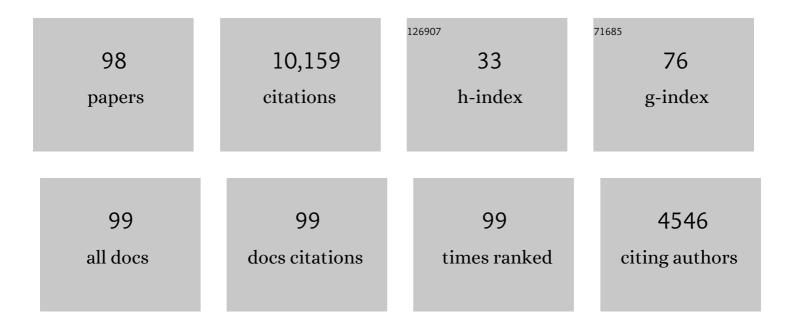
List of Publications by Year in descending order

Source: https://exaly.com/author-pdf/3574417/publications.pdf Version: 2024-02-01



SHIDO KEDA

#	Article	IF	CITATIONS
1	The Variability of the Black Hole Image in M87 at the Dynamical Timescale. Astrophysical Journal, 2022, 925, 13.	4.5	6
2	First Sagittarius A* Event Horizon Telescope Results. III. Imaging of the Galactic Center Supermassive Black Hole. Astrophysical Journal Letters, 2022, 930, L14.	8.3	163
3	Characterizing and Mitigating Intraday Variability: Reconstructing Source Structure in Accreting Black Holes with mm-VLBI. Astrophysical Journal Letters, 2022, 930, L21.	8.3	20
4	First Sagittarius A* Event Horizon Telescope Results. VI. Testing the Black Hole Metric. Astrophysical Journal Letters, 2022, 930, L17.	8.3	215
5	First Sagittarius A* Event Horizon Telescope Results. II. EHT and Multiwavelength Observations, Data Processing, and Calibration. Astrophysical Journal Letters, 2022, 930, L13.	8.3	142
6	First Sagittarius A* Event Horizon Telescope Results. IV. Variability, Morphology, and Black Hole Mass. Astrophysical Journal Letters, 2022, 930, L15.	8.3	137
7	First Sagittarius A* Event Horizon Telescope Results. I. The Shadow of the Supermassive Black Hole in the Center of the Milky Way. Astrophysical Journal Letters, 2022, 930, L12.	8.3	568
8	Selective Dynamical Imaging of Interferometric Data. Astrophysical Journal Letters, 2022, 930, L18.	8.3	21
9	Millimeter Light Curves of Sagittarius A* Observed during the 2017 Event Horizon Telescope Campaign. Astrophysical Journal Letters, 2022, 930, L19.	8.3	43
10	A Universal Power-law Prescription for Variability from Synthetic Images of Black Hole Accretion Flows. Astrophysical Journal Letters, 2022, 930, L20.	8.3	20
11	First Sagittarius A* Event Horizon Telescope Results. V. Testing Astrophysical Models of the Galactic Center Black Hole. Astrophysical Journal Letters, 2022, 930, L16.	8.3	187
12	First M87 Event Horizon Telescope Results. VII. Polarization of the Ring. Astrophysical Journal Letters, 2021, 910, L12.	8.3	215
13	First M87 Event Horizon Telescope Results. VIII. Magnetic Field Structure near The Event Horizon. Astrophysical Journal Letters, 2021, 910, L13.	8.3	297
14	Noise reduction for weak lensing mass mapping: an application of generative adversarial networks to Subaru Hyper Suprime-Cam first-year data. Monthly Notices of the Royal Astronomical Society, 2021, 504, 1825-1839.	4.4	15
15	Broadband Multi-wavelength Properties of M87 during the 2017 Event Horizon Telescope Campaign. Astrophysical Journal Letters, 2021, 911, L11.	8.3	56
16	Extracting common signal components from the X-ray and optical light curves of GX 339â^'4: New view for anti-correlation. Publication of the Astronomical Society of Japan, 2021, 73, 716-727.	2.5	0
17	Constraints on black-hole charges with the 2017 EHT observations of M87*. Physical Review D, 2021, 103, .	4.7	126
18	The Polarized Image of a Synchrotron-emitting Ring of Gas Orbiting a Black Hole. Astrophysical Journal, 2021, 912, 35.	4.5	43

#	Article	IF	CITATIONS
19	Three-dimensional Reconstruction of Weak-lensing Mass Maps with a Sparsity Prior. I. Cluster Detection. Astrophysical Journal, 2021, 916, 67.	4.5	2
20	Event Horizon Telescope observations of the jet launching and collimation in Centaurus A. Nature Astronomy, 2021, 5, 1017-1028.	10.1	65
21	A Data-scientific Noise-removal Method for Efficient Submillimeter Spectroscopy With Single-dish Telescopes. Astronomical Journal, 2021, 162, 111.	4.7	4
22	ALMA Super-resolution Imaging of T Tau: r = 12 au Gap in the Compact Dust Disk around T Tau N. Astrophysical Journal, 2021, 923, 121.	4.5	6
23	An optical search for transients lasting a few seconds. Publication of the Astronomical Society of Japan, 2020, 72, .	2.5	5
24	Relationship between radar cross section and optical magnitude based on radar and optical simultaneous observations of faint meteors. Planetary and Space Science, 2020, 194, 105011.	1.7	4
25	Feature selection for classification of blazars based on optical photometric and polarimetric time-series data. Publication of the Astronomical Society of Japan, 2020, 72, .	2.5	1
26	Super-resolution Imaging of the Protoplanetary Disk HD 142527 Using Sparse Modeling. Astrophysical Journal, 2020, 895, 84.	4.5	7
27	Amino-acid selective isotope labeling enables simultaneous overlapping signal decomposition and information extraction from NMR spectra. Journal of Biomolecular NMR, 2020, 74, 125-137.	2.8	2
28	Event Horizon Telescope imaging of the archetypal blazar 3C 279 at an extreme 20 microarcsecond resolution. Astronomy and Astrophysics, 2020, 640, A69.	5.1	54
29	SYMBA: An end-to-end VLBI synthetic data generation pipeline. Astronomy and Astrophysics, 2020, 636, A5.	5.1	18
30	Search for Alignment of Disk Orientations in Nearby Star-forming Regions: Lupus, Taurus, Upper Scorpius, ϕOphiuchi, and Orion. Astrophysical Journal, 2020, 899, 55.	4.5	7
31	The Event Horizon General Relativistic Magnetohydrodynamic Code Comparison Project. Astrophysical Journal, Supplement Series, 2019, 243, 26.	7.7	175
32	Concept for an X-ray telescope system with an angular resolution booster. Publication of the Astronomical Society of Japan, 2019, 71, .	2.5	0
33	Denoising weak lensing mass maps with deep learning. Physical Review D, 2019, 100, .	4.7	17
34	The Hyper Suprime-Cam SSP transient survey in COSMOS: Overview. Publication of the Astronomical Society of Japan, 2019, 71, .	2.5	22
35	An image reconstruction method for an X-ray telescope system with an angular resolution booster. Publication of the Astronomical Society of Japan, 2019, 71, .	2.5	2
36	Luminosity function of faint sporadic meteors measured with a wide-field CMOS mosaic camera Tomo-e PM. Planetary and Space Science, 2019, 165, 281-292.	1.7	3

#	Article	IF	CITATIONS
37	First M87 Event Horizon Telescope Results. III. Data Processing and Calibration. Astrophysical Journal Letters, 2019, 875, L3.	8.3	519
38	First M87 Event Horizon Telescope Results. II. Array and Instrumentation. Astrophysical Journal Letters, 2019, 875, L2.	8.3	618
39	First M87 Event Horizon Telescope Results. IV. Imaging the Central Supermassive Black Hole. Astrophysical Journal Letters, 2019, 875, L4.	8.3	806
40	First M87 Event Horizon Telescope Results. I. The Shadow of the Supermassive Black Hole. Astrophysical Journal Letters, 2019, 875, L1.	8.3	2,264
41	First M87 Event Horizon Telescope Results. V. Physical Origin of the Asymmetric Ring. Astrophysical Journal Letters, 2019, 875, L5.	8.3	814
42	First M87 Event Horizon Telescope Results. VI. The Shadow and Mass of the Central Black Hole. Astrophysical Journal Letters, 2019, 875, L6.	8.3	897
43	New Constraint on the Atmosphere of (50000) Quaoar from a Stellar Occultation. Astronomical Journal, 2019, 158, 236.	4.7	10
44	Superresolution Interferometric Imaging with Sparse Modeling Using Total Squared Variation: Application to Imaging the Black Hole Shadow. Astrophysical Journal, 2018, 858, 56.	4.5	43
45	Exhaustive Search for Sparse Variable Selection in Linear Regression. Journal of the Physical Society of Japan, 2018, 87, 044802.	1.6	35
46	"Slow-scanning―in Ground-based Mid-infrared Observations. Astrophysical Journal, 2018, 857, 37.	4.5	6
47	The Tomo-e Gozen wide field CMOS camera for the Kiso Schmidt telescope. , 2018, , .		22
48	Evaluation of large pixel CMOS image sensors for the Tomo-e Gozen wide field camera. , 2018, , .		5
49	New method of eclipse mapping and an application to HT Cas in the 2017 superoutburst. , 2018, , .		Ο
50	DATA COMPRESSION FOR THE TOMO-e GOZEN USING LOW-RANK MATRIX APPROXIMATION. Astrophysical Journal, 2017, 835, 1.	4.5	19
51	Imaging the Schwarzschild-radius-scale Structure of M87 with the Event Horizon Telescope Using Sparse Modeling. Astrophysical Journal, 2017, 838, 1.	4.5	111
52	Superresolution Full-polarimetric Imaging for Radio Interferometry with Sparse Modeling. Astronomical Journal, 2017, 153, 159.	4.7	70
53	Accelerating cross-validation with total variation and its application to super-resolution imaging. PLoS ONE, 2017, 12, e0188012.	2.5	5
54	Protein NMR Structure Refinement based on Bayesian Inference. Journal of Physics: Conference Series, 2016, 699, 012005.	0.4	10

#	Article	IF	CITATIONS
55	Data-driven approach to Type Ia supernovae: variable selection on the peak luminosity and clustering in visual analytics. Journal of Physics: Conference Series, 2016, 699, 012009.	0.4	2
56	Rate–Distortion Functions for Gamma-Type Sources Under Absolute-Log Distortion Measure. IEEE Transactions on Information Theory, 2016, 62, 5496-5502.	2.4	2
57	Development of a prototype of the Tomo-e Gozen wide-field CMOS camera. Proceedings of SPIE, 2016, , .	0.8	12
58	Improved in-cell structure determination of proteins at near-physiological concentration. Scientific Reports, 2016, 6, 38312.	3.3	43
59	An asymmetric logistic regression model for ecological data. Methods in Ecology and Evolution, 2016, 7, 249-260.	5.2	31
60	Development of a real-time data processing system for a prototype of the Tomo-e Gozen wide field CMOS camera. Proceedings of SPIE, 2016, , .	0.8	3
61	Sparse Modeling for Astronomical Data Analysis. Journal of Physics: Conference Series, 2016, 699, 012008.	0.4	0
62	PRECL: A new method for interferometry imaging from closure phase. Publication of the Astronomical Society of Japan, 2016, 68, .	2.5	17
63	Imaging black holes with sparse modeling. Journal of Physics: Conference Series, 2016, 699, 012006.	0.4	8
64	Risk assessment of radioisotope contamination for aquatic living resources in and around Japan. Proceedings of the National Academy of Sciences of the United States of America, 2016, 113, 3838-3843.	7.1	35
65	Variable selection for modeling the absolute magnitude at maximum of TypeÂla supernovae. Publication of the Astronomical Society of Japan, 2015, 67, .	2.5	13
66	Sparsely extracting stored movements to construct interfaces for humanoid end-effector control. , 2015, , .		0
67	Entropic risk minimization for nonparametric estimation of mixing distributions. Machine Learning, 2015, 99, 119-136.	5.4	3
68	Super-resolution imaging with radio interferometry using sparse modeling. Publication of the Astronomical Society of Japan, 2014, 66, .	2.5	73
69	Bin mode estimation methods for Compton camera imaging. Nuclear Instruments and Methods in Physics Research, Section A: Accelerators, Spectrometers, Detectors and Associated Equipment, 2014, 760, 46-56.	1.6	10
70	Compton camera imaging. , 2013, , .		1
71	Rate-distortion function for gamma sources under absolute-log distortion measure. , 2013, , .		4
72	Introduction to the issue on differential geometry in signal processing. IEEE Journal on Selected Topics in Signal Processing, 2013, 7, 573-575.	10.8	5

#	Article	IF	CITATIONS
73	Phase retrieval from single biomolecule diffraction pattern. Optics Express, 2012, 20, 3375.	3.4	12
74	Channel Capacity and Optimization of Probability Measure. leice Ess Fundamentals Review, 2012, 5, 230-238.	0.1	0
75	Editorial - Neural Networks and Learning Systems Come Together. IEEE Transactions on Neural Networks and Learning Systems, 2012, 23, 1-6.	11.3	6
76	An introductory review of information theory in the context of computational neuroscience. Biological Cybernetics, 2011, 105, 55-70.	1.3	26
77	Combining binary machines for multi-class: Statistical model and parameter estimation. Journal of Physics: Conference Series, 2010, 233, 012006.	0.4	0
78	Motor planning as an optimization of command representation. , 2009, , .		4
79	Spiking neuron channel. , 2009, , .		2
80	Capacity of a Single Spiking Neuron Channel. Neural Computation, 2009, 21, 1714-1748.	2.2	39
81	Capacity of a single spiking neuron. Journal of Physics: Conference Series, 2009, 197, 012014.	0.4	0
82	Channel Estimation and Code Word Inference for Mobile Digital Satellite Broadcasting Reception. IEICE Transactions on Communications, 2008, E91-B, 3886-3898.	0.7	0
83	Improving Mobile Reception of Digital Satellite Broadcasting. , 2007, , .		0
84	Motor planning and sparse motor command representation. Neurocomputing, 2007, 70, 1748-1752.	5.9	4
85	Information geometry for turbo decoding. Systems and Computers in Japan, 2005, 36, 79-87.	0.2	2
86	Stochastic Reasoning, Free Energy, and Information Geometry. Neural Computation, 2004, 16, 1779-1810.	2.2	48
87	Information Geometry of Turbo and Low-Density Parity-Check Codes. IEEE Transactions on Information Theory, 2004, 50, 1097-1114.	2.4	43
88	Combined approach of array processing and independent component analysis for blind separation of acoustic signals. IEEE Transactions on Speech and Audio Processing, 2003, 11, 204-215.	1.5	97
89	An approach to blind source separation based on temporal structure of speech signals. Neurocomputing, 2001, 41, 1-24.	5.9	502
90	Independent component analysis for noisy data — MEG data analysis. Neural Networks, 2000, 13, 1063-1074.	5.9	109

#	Article	IF	CITATIONS
91	ICA for noisy neurobiological data. , 2000, , .		2
92	ICA on Noisy Data: A Factor Analysis Approach. Perspectives in Neural Computing, 2000, , 201-215.	0.1	12
93	A robot organizing purposive behavior by itself. , 0, , .		3
94	A self-organizing system with cell-specialization. , 0, , .		2
95	A combined approach of array processing and independent component analysis for blind separation of acoustic signals. , 0, , .		30
96	Information geometry of turbo codes. , 0, , .		2
97	Information geometry of turbo and LDPC codes. , 0, , .		1
98	Machine-learning selection of optical transients in the Subaru/Hyper Suprime-Cam survey. Publication of the Astronomical Society of Japan, 0, , .	2.5	28